

# Busbar protection scheme based on alienation coefficients for current signals

R. Abd Allah

Buraydah Colleges, Faculty of Engineering, Electrical Power Department, Qassim Region, Kingdom of Saudi Arabia

**Email address:**

Mohandes\_Ragab@yahoo.com

**To cite this article:**

R. Abd Allah. Busbar Protection Scheme Based on Alienation Coefficients for Current Signals. *International Journal of Energy and Power Engineering*. Vol. 3, No. 3, 2014, pp. 103-115. doi: 10.11648/j.ijepe.20140303.11

---

**Abstract:** In modern digital power system protection systems, statistical coefficients technique is recently used for fault analysis. An alienation technique is developed for busbar protection against all ten types of shunt faults, which may locate in busbar protection zone, under different loading levels, fault resistances and fault inception angle. It does not need any extra equipment as it depends only on the three-line currents measurements, of all feeders connected to the protected busbar, which are mostly available at the relay location. It is able to perform fault detection, fault confirmation, faulty phase selection and determine the fault location in about a half-cycle period. Thus, the alienation technique is well suited for implementation in digital protection schemes. The technique is efficient to detect current transformer saturation conditions without needing any additional algorithm. The effects of DC components and harmonics are eliminated with estimation of alienation coefficients. The proposed methodology is applied for a part of 500 KV Egyptian network. Alternative transient program (ATP) and MATLAB package are used to implement the proposed technique.

**Keywords:** Busbar Protection, Current Transformer Saturation, Fault Detection, Internal and External Faults, Alienation Coefficient, ATP Software, MATLAB

---

## 1. Introduction

A busbar is a critical element of a power system, as it is the point of convergence of many circuits, transmission, generation, or loads. The effect of a single bus fault is equivalent to many simultaneous faults and usually, due to the concentration of supply circuits, involves high current magnitudes. High-speed busbar protection is often required to limit the damaging effects on equipment and system stability or to maintain service to as much load as possible. Differential protection is the most sensitive and reliable method for protecting a station buses. The phasor summation of all the measured current entering and leaving the bus must be zero unless there is a fault within the protective zone. For a fault not in the protective zone, the faulted circuit is energized at a much higher level, near CT saturation or with varying degrees of CT saturation, giving rise to possible high false differential currents. Under ideal conditions, the secondary current developed by CT will be the primary current divided by the CT turns ratio. However, the CT secondary current will not be a sine wave when the flux in the CT core reaches into the saturated region. The factors affecting this are secondary burden, primary current

magnitude, asymmetry in the primary current, remanent flux in the CT core, saturation voltage, fault inception angle and CT turns ratio [1]. Actually, the DC component has far more influence in producing severe saturation than the AC fault current. Direct current saturation is particularly significant in bus differential relaying systems, where highly differing currents flow to an external fault through the current transformers of the various circuits. Dissimilar saturation in any differential scheme will produce operating current. The problem of CT saturation is not popular in case of an internal fault conditions. Severe current transformer saturation will occur if the primary circuit DC time constant is sufficiently long and the DC component sufficiently high. The DC component arises because the current in an inductance cannot change instantaneously and the steady- state current, before and after a change, must lag (or lead) the voltage by the proper power- factor angle. Many methods are used to avoid the CT saturation. The problem of CT saturation is eliminated by air-core CT's called "linear couplers". In fact, these CT's have a disadvantage that very little current can be drawn from the secondary, because so much of the primary magneto-motive force is consumed in magnetizing the core.

Another method is used to increase the size of the CT core to obtain a higher saturation voltage than a calculated value [2]. Another one uses special core material to withstand large flux density [3]. These options present mechanical and economic difficulties. Recently, many software techniques are provided to solve these problems and each method has its advantage and disadvantage. Some techniques use a DC component equal and opposite to that in the primary circuit generated by a circuit added to the secondary winding [4]. Other techniques use a magnetization curve and the equivalent circuit of a CT for compensating secondary current of CT during saturation condition; these techniques have practical difficulties, as it depends on CT parameters /characteristics and secondary burdens [5]. Also, Artificial Neural Networks (ANNs) are used in this area to learn the nonlinear characteristics of CT magnetization and restructures the waveform based on the learned characteristics. This method could not be applied to different CT's due to the variations of CT's saturation characteristics and the secondary burdens [6]. Some other algorithms prevent relay operation during CT saturation [7]. This may result in longer trip times. A method for compensating the secondary current of CT's is based on the ideal proportional transient secondary fault current. A portion of measured secondary current following the fault occurrence is described using regression analysis [8]. Another method utilizes four consequent samples, during the unsaturated portion of each cycle, for solving a set of equations to obtain the constants of the primary fault current equation for re-constructing the secondary current during the saturated part. The scheme calculates the correct primary time constant by repeating the calculations of the algorithm using different values of time constant and chooses the value that gives the smallest error [9]. A digital technique for protecting busbars presented in [10] uses positive- and negative-sequence models of the power system in a fault-detection algorithm. While phase voltages and currents are used to detect faults, parameters of the power system are not used. Another method called current phase comparison is presented in [11], which can achieve reliable busbar protection with minimum CT performance requirements. Thousands of RTDS test and MATLAB analyses have been performed, which proved that the stability of busbar protection can be greatly improved by this algorithm. The presented principle in paper [12] describes a methodology for protecting busbars. The method uses the ratio between the fault component voltage and the fault component differential current of the busbar to detect faults, which is defined as the fault component integrated impedance. The fault component integrated impedance of an external fault reflects the capacitance impedance of the busbar whereas that of an internal fault reflects the parallel connection result of the impedances of all the feeders connected to the busbar. As a result, the magnitudes of the integrated impedances are quite different between an external fault and an internal fault. A model parameter identification based bus-bar protection principle

is proposed in paper [13]. An inductance model can be developed when an internal fault occurs on bus. By taking the inductance and the resistance of the model as the unknown parameters to be identified, the equivalent instantaneous impedance and the dispersion of the parameter can be calculated. Utilizing their difference, the external fault and the internal fault with different current transformer (CT) saturation extent can be distinguished. Through-out this work a new technique for busbar protection based on alienation coefficients is suggested. The technique measures the three-line currents of each feeder connected to the protected busbar, which are mostly available at the relay location. The alienation coefficient is calculated between input and output currents of each phase for busbar in order to make relay trip or no trip decision. The suggested technique takes into consideration the wide variations of operating conditions such as loading levels, fault resistance and fault inception angle.

## 2. Proposed Technique

### 2.1. Basic Principles

In this paper, ATP software [14] is used to get reliable simulation results before and during different fault conditions which are located in and out the protective zone of busbar. Three-phase current signals of each feeder, connected to the busbar, are obtained and stored in a file; this data is in the discrete sampled form. These current samples are processed in MATLAB to get alienation coefficients [15-16] estimated between the input and output phase current signals of the busbar. The suggested technique is based on alienation concept in order to determine busbar fault type whether internal or external to make relay trip or no trip decision, respectively. The calculations of the alienation coefficients are processed for each two corresponding quarter-cycles of the two currents to get high-speed operation for busbar protection.

### 2.2. Alienation Coefficients Calculation

The variance between any two signals is defined as the alienation coefficient [17-19], which is obtained from correlation coefficient; thus alienation coefficient is a good proposed technique for making busbar protection against different fault conditions located on the busbar element. Alienation coefficient calculated between the two phase currents entering and leaving the bus can recognize a variance between them and to operate in response to it. This coefficient is derived from cross-correlation coefficient. Cross-correlation coefficient ( $r_a$ ) is calculated between each two corresponding windows of the two sampled currents ( $i_{a1}$  and  $i_{a2}$ ) entering and leaving the phase "A" bus, where the two windows are shifted from each other with a time interval  $h\Delta t$ . The coefficient ( $r_a$ ) between the two signals ( $i_{a1}$  and  $i_{a2}$ ) is given by Equation (1). Our proposed technique uses the two signals shifted from each other when the time interval  $h\Delta t = 0$ , where  $h =$

0 ( $h$  is the number of samples between the two windows which are shifted from each other and  $\Delta t$  is the time interval of one sample). Also cross-correlation coefficients ( $r_b$  and  $r_c$ ) are given by Equations (2) and (3), respectively.

$$r_a = \frac{\sum_{k=1}^m i_{a1}(k) i_{a2}(k+h\Delta t) - \frac{1}{m} \sum_{k=1}^m i_{a1}(k) \sum_{k=1}^m i_{a2}(k+h\Delta t)}{\sqrt{\left(\sum_{k=1}^m i_{a1}(k)^2 - \frac{1}{m} \left(\sum_{k=1}^m i_{a1}(k)\right)^2\right) \times \left(\sum_{k=1}^m i_{a2}(k+h\Delta t)^2 - \frac{1}{m} \left(\sum_{k=1}^m i_{a2}(k+h\Delta t)\right)^2\right)}} \quad (1)$$

$$r_b = \frac{\sum_{k=1}^m i_{b1}(k) i_{b2}(k+h\Delta t) - \frac{1}{m} \sum_{k=1}^m i_{b1}(k) \sum_{k=1}^m i_{b2}(k+h\Delta t)}{\sqrt{\left(\sum_{k=1}^m i_{b1}(k)^2 - \frac{1}{m} \left(\sum_{k=1}^m i_{b1}(k)\right)^2\right) \times \left(\sum_{k=1}^m i_{b2}(k+h\Delta t)^2 - \frac{1}{m} \left(\sum_{k=1}^m i_{b2}(k+h\Delta t)\right)^2\right)}} \quad (2)$$

$$r_c = \frac{\sum_{k=1}^m i_{c1}(k) i_{c2}(k+h\Delta t) - \frac{1}{m} \sum_{k=1}^m i_{c1}(k) \sum_{k=1}^m i_{c2}(k+h\Delta t)}{\sqrt{\left(\sum_{k=1}^m i_{c1}(k)^2 - \frac{1}{m} \left(\sum_{k=1}^m i_{c1}(k)\right)^2\right) \times \left(\sum_{k=1}^m i_{c2}(k+h\Delta t)^2 - \frac{1}{m} \left(\sum_{k=1}^m i_{c2}(k+h\Delta t)\right)^2\right)}} \quad (3)$$

Where,

$r_a$ : The cross-correlation coefficient calculated between input and output current signals ( $i_{a1}$  and  $i_{a2}$ ) for the phase "A" of busbar.

$r_b$ : The cross-correlation coefficient calculated between input and output current signals ( $i_{b1}$  and  $i_{b2}$ ) for the phase "B" of busbar.

$r_c$ : The cross-correlation coefficient calculated between input and output current signals ( $i_{c1}$  and  $i_{c2}$ ) for the phase "C" of busbar.

$m$ : the number of samples per window to be correlated used in the algorithm (the number of samples per quarter-cycle are selected in the algorithm,  $m = N/4 = 100/4 = 25$  samples).

$i_{a1}(k)$ : the summation input current values at instant  $k$  for phase "A" of busbar.

$i_{a2}(k)$ : the summation output current values at instant  $k$  for phase "A" of busbar.

$i_{b1}(k)$ : the summation input current values at instant  $k$  for phase "B" of busbar.

$i_{b2}(k)$ : the summation output current values at instant  $k$  for phase "B" of busbar.

$i_{c1}(k)$ : the summation input current values at instant  $k$  for phase "C" of busbar.

$i_{c2}(k)$ : the summation output current values at instant  $k$  for phase "C" of busbar.

The alienation coefficient ( $A_a$ ), calculated between the two current signals ( $i_{a1}$  and  $i_{a2}$ ), is obtained from cross-correlation coefficient ( $r_a$ ) and it is given in Equation (4). Also alienation coefficients ( $A_b$  and  $A_c$ ) are given by Equations (5) and (6), respectively.

$$A_a = 1 - (r_a)^2 \quad (4)$$

$$A_b = 1 - (r_b)^2 \quad (5)$$

$$A_c = 1 - (r_c)^2 \quad (6)$$

Where,

$A_a$ : The alienation coefficient calculated between the two current signals ( $i_{a1}$  and  $i_{a2}$ ) for the phase "A" of busbar.

$A_b$ : The alienation coefficient calculated between the two current signals ( $i_{b1}$  and  $i_{b2}$ ) for the phase "B" of busbar.

$A_c$ : The alienation coefficient calculated between the two current signals ( $i_{c1}$  and  $i_{c2}$ ) for the phase "C" of busbar.

Correlation and alienation coefficients are a dimensionless quantities and it does not depend on the units employed. The value of cross-correlation is between "-1" and "1", this produces the value of alienation coefficient to be between "0" and "1".

### 2.3. Busbar Protection Procedures

Flow chart for busbar protection algorithm based on alienation technique is shown in Fig. 1. The algorithm has the following procedures:

1- Read discrete sampled of three-phase secondary current signals for three-phase current transformers of each feeder connected to the protected busbar (obtained from ATP tool).

2- Calculate input and output current values ( $i_{a1}(k)$ ,  $i_{a2}(k)$ ,  $i_{b1}(k)$ ,  $i_{b2}(k)$ ,  $i_{c1}(k)$  and  $i_{c2}(k)$ ) for each phase of the protected busbar.

3- Calculate cross-correlation coefficient calculated between the input and output current signals for each phase of busbar as given by Equations (7), (8) and (9),

$$r_a = \frac{\sum_{k=1}^m i_{a1}(k) i_{a2}(k) - \frac{1}{m} \sum_{k=1}^m i_{a1}(k) \sum_{k=1}^m i_{a2}(k)}{\sqrt{\left(\sum_{k=1}^m i_{a1}(k)^2 - \frac{1}{m} \left(\sum_{k=1}^m i_{a1}(k)\right)^2\right) \times \left(\sum_{k=1}^m i_{a2}(k)^2 - \frac{1}{m} \left(\sum_{k=1}^m i_{a2}(k)\right)^2\right)}} \quad (7)$$

$$r_b = \frac{\sum_{k=1}^m i_{b1}(k) i_{b2}(k) - \frac{1}{m} \sum_{k=1}^m i_{b1}(k) \sum_{k=1}^m i_{b2}(k)}{\sqrt{\left(\sum_{k=1}^m i_{b1}(k)^2 - \frac{1}{m} \left(\sum_{k=1}^m i_{b1}(k)\right)^2\right) \times \left(\sum_{k=1}^m i_{b2}(k)^2 - \frac{1}{m} \left(\sum_{k=1}^m i_{b2}(k)\right)^2\right)}} \quad (8)$$

$$r_c = \frac{\sum_{k=1}^m i_{c1}(k) i_{c2}(k) - \frac{1}{m} \sum_{k=1}^m i_{c1}(k) \sum_{k=1}^m i_{c2}(k)}{\sqrt{\left(\sum_{k=1}^m i_{c1}(k)^2 - \frac{1}{m} \left(\sum_{k=1}^m i_{c1}(k)\right)^2\right) \times \left(\sum_{k=1}^m i_{c2}(k)^2 - \frac{1}{m} \left(\sum_{k=1}^m i_{c2}(k)\right)^2\right)}} \quad (9)$$

4- Calculate the alienation coefficients ( $A_a$ ,  $A_b$  and  $A_c$ ), by using the calculated cross-correlation coefficients ( $r_a$ ,  $r_b$  and  $r_c$ ), respectively as given in Equations (4), (5) and (6).

In case of no internal fault condition, it is known that the total sum of input currents is equal to the total sum of output currents for each phase of busbar. Alienation coefficient, calculated between the input and output currents for each phase, must be zero unless there is a fault within the busbar protective zone. Thus it is developed for faults detection, fault confirmation, and faulty phase selection in our proposed scheme. The proposed technique

is able to accurately identify the condition of phase(s) involved in all ten types of shunt faults that may occur in busbars under different loading levels, fault resistances and fault inception angles. Our proposed algorithm calculates the three-phase alienation coefficients ( $A_a$ ,  $A_b$  and  $A_c$ ); Normally, the value of cross-correlation coefficient is "1" because the phase shift is  $0^\circ$  in case of ideal normal operation or external fault without CT saturation ( $r_a = r_b = r_c = \cos(0^\circ) = 1$ ), hence ( $A_a = A_b = A_c = 1 - (\cos(0^\circ))^2 = 0.0$ ). In cases of internal faults located on the protected busbar, the previous rule is not verified. No ideal operation condition in power system. To avoid this drawback, operation under healthy condition is restricted by alienation coefficients limits ( $A_x$ ), where,  $A_x = 0.05$ .

#### 5- Fault detection and faulty phase selection

To implement our technique, three tasks are starting in parallel: fault detection, fault confirmation, and faulty phase selection as follows:

##### Fault detection (initiation)

A transition is detected for each phase of busbar if:  $\Delta I > 20\% I_n$ , where  $I_n$  is the busbar nominal current.

##### Faulty phase selection

- Fault confirmation and faulty phase selection are done according to the following sequences:

Three-phase current alienation coefficients values ( $A_a$ ,  $A_b$  and  $A_c$ ) are calculated. If fault is detected, phase current alienation values are sorted and compared. The possible fault cases are:

(a) If the three-phase alienation coefficients values are equal or less than  $A_x$ , where the selected  $A_x$  is 0.05, then the condition is external fault or normal operation.

- If  $A_a \leq A_x$ ,  $A_b \leq A_x$  and  $A_c \leq A_x$ , the fault type is external or normal operation.

(b) If the three-phase alienation coefficients values are greater than  $A_x$ , then the fault is three-phase and internal.

- If  $A_a > A_x$ ,  $A_b > A_x$  and  $A_c > A_x$ , the fault is three-phase and internal (a-b-c fault).

(c) If the two-phase alienation coefficients values are nearly zero (or equal or less than  $A_x$ ), while the third phase alienation coefficient is greater than  $A_x$ , the fault is internal single phase-to-ground.

- If  $A_a > A_x$ ,  $A_b \leq A_x$ ,  $A_c \leq A_x$ , the fault is single phase-to-ground and internal (a-g fault).

- If  $A_b > A_x$ ,  $A_a \leq A_x$ ,  $A_c \leq A_x$ , the fault is single phase-to-ground and internal (b-g fault).

- If  $A_c > A_x$ ,  $A_a \leq A_x$ ,  $A_b \leq A_x$ , the fault is single phase-to-ground and internal (c-g fault).

(d) If the two-phase alienation coefficients values are greater than  $A_x$ , while the third phase alienation coefficient is equal or less than  $A_x$ , the fault is internal and it may be phase-to-phase or double phase-to-ground and internal.

- If  $A_a > A_x$ ,  $A_b > A_x$ ,  $A_c \leq A_x$ , the fault is internal and it may be phase-to-phase (a-b fault) or double phase-to-ground (a-b-g fault).

- If  $A_a \leq A_x$ ,  $A_b > A_x$ ,  $A_c > A_x$ , the fault is internal and it may be phase-to-phase (b-c fault) or double phase-to-ground (b-c-g fault).

- If  $A_a > A_x$ ,  $A_b \leq A_x$ ,  $A_c > A_x$ , the fault is internal and it may be phase-to-phase (a-c fault) or double phase-to-ground (a-c-g fault).

(e) To make sure of distinguishing between double phase and double phase-to-ground faults, the alienation coefficient is calculated between the two faulted phase's currents for the input (or output) phase currents of the protected busbar. If the value of alienation is nearly zero, the fault is phase-to-phase.

- If  $A_{ab} \leq A_x$  the fault is phase-to-phase and internal (a-b fault) otherwise the fault is double phase-to-ground and internal (a-b-g fault).

- If  $A_{bc} \leq A_x$  the fault is phase-to-phase and internal (b-c fault) otherwise the fault is double phase-to-ground and internal (b-c-g fault).

- If  $A_{ac} \leq A_x$  the fault is phase-to-phase and internal (a-c fault) otherwise the fault is double phase-to-ground and internal (a-c-g fault).

6- Tripping/blocking action of the algorithm relies on the following rules for the following conditions:

(a) Normal operation condition,

- If  $A_a \leq A_x$ ,  $A_b \leq A_x$  and  $A_c \leq A_x$  (for each phase of busbar), then this case is (healthy) normal operation or external fault without CT saturation condition (where,  $A_x = 0.05$  is selected) and the scheme holds trip signal to low (0).

-  $A_a \approx A_b \approx A_c \leq A_x$

(b) Internal fault condition

- If  $A_a > A_x$ ,  $A_b > A_x$  or  $A_c > A_x$  (for any phase of the protected busbar), then this case indicates to internal fault condition inside the protective busbar zone. Hence the faulted busbar must be isolated from the remaining power system, and the scheme sets trip signal to high (1).

-  $T_{bb} = 0 \text{ Sec}$ , where,  $T_{bb}$  = Operating time (in Sec) for busbar protection function.

(c) External fault with CT saturation condition

- If  $A_a \leq A_x$ ,  $A_b \leq A_x$  and  $A_c \leq A_x$  during the first quarter-cycle after fault detection because of the free saturated portion of secondary current signals, then this case is external fault with CT saturation condition. In this condition, the alienation coefficient is greater than  $A_x$  during the distorted portions of current signal and it is less than  $A_x$  during unsaturated portions. This event makes the scheme holds trip signal to low (0). The fault type's conditions, alienation coefficient limits and relay action are given in Table 1.

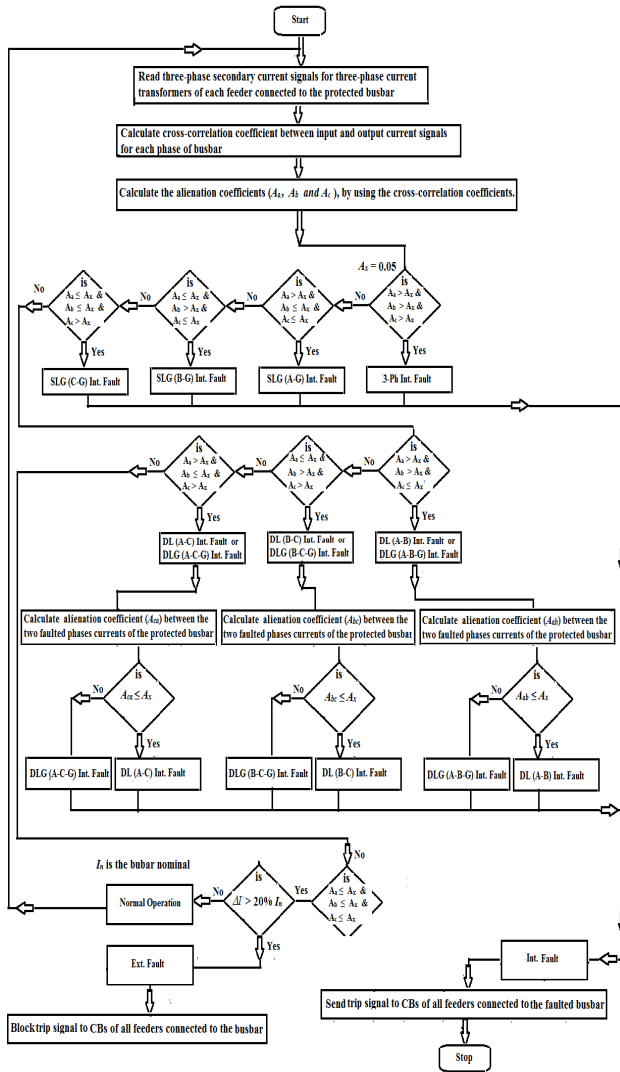


**Figure 1.** Flow Chart for Busbar Protection Algorithm Based on Alienation Technique.

**Table 1.** Alienation coefficient ranges at different fault conditions for the protected busbar.

Fault Type	Alienation Coefficients $A_x = 0.05$	Relay Action
1. Normal (healthy) condition	$A_a \leq A_x, A_b \leq A_x \text{ and } A_c \leq A_x$	Blocking
2. External fault condition (without CT saturation)	$A_a \leq A_x, A_b \leq A_x \text{ and } A_c \leq A_x$	Blocking
3. Internal fault condition	$A_a > A_x, A_b > A_x \text{ or } A_c > A_x$	Tripping
4. External fault condition (with CT saturation)	$A_a \leq A_x, A_b \leq A_x \text{ and } A_c \leq A_x$ (During the first quarter-cycle after fault detection, i.e. free saturated portion of secondary current signals)	Blocking

a part of the Egyptian 500 KV unified network [20] and are given in Table 2.

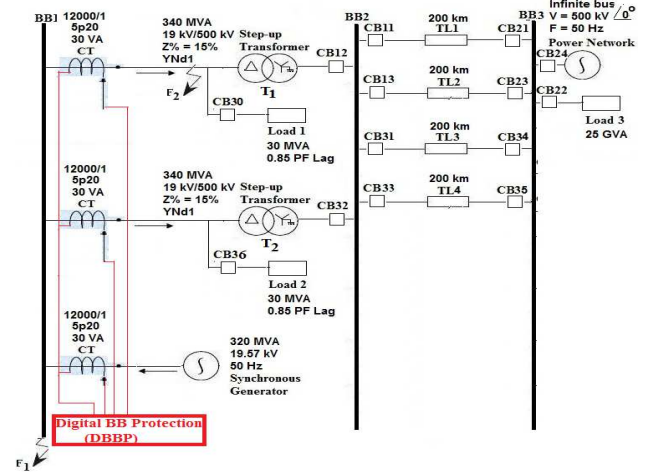


**Figure 2.** Single Line Diagram for the Studied Power System.

**Table 2.** Power system parameters data

Power system parameter	Data
<b>Synchronous Generator (Sending source):</b>	
Rated Volt-ampere / Rated line voltage	320 MVA / 19.57 kV / 50 Hz
/ Rated frequency	
Number of poles /Neutral grounding impedance ( $R_n$ )	2/ 0.77 ohm
<b>Step-up Transformer:</b>	
Rated Volt-ampere	340 MVA
Transformation voltage ratio	Delta/Star earthed neutral
Connection primary/secondary	0.0027 + j 0.184 ohm
Primary winding impedance ( $Z_p$ )	0.7708 + j 61.8 ohm.
Secondary winding impedance ( $Z_s$ )	
Vector group	YNd1
Z%	15%
<b>Transmission Lines:</b>	
+ve sequence R	0.0217ohm /km
Zero sequence R	0.247 ohm/km
+ve sequence XL	0.302 ohm/km
Zero sequence XL	0.91 ohm/km
+ve sequence 1/Xc	3.96 micro-mho /km
Zero sequence 1/Xc	2.94 micro-mho /km
Transmission line long (Km)	200 Km
<b>Aux. Load (load 1):</b>	
Load 1 Volt-ampere	30 MVA at PF = 0.85 lag
<b>Aux. Load (load 2):</b>	
Load 2 Volt-ampere	30 MVA at PF = 0.85 lag
<b>Power Network (Receiving source):</b>	
Nominal line voltage	500kV (1pu)
Voltage phasor angle phase	0°
Nominal frequency	50 Hz
Volt-ampere short circuit	25 GVA ( $i_{sc} = 10 \text{ kA}$ )
<b>Current Transformer (CT):</b>	
CTR	12000 A/ 1A
Rated burden	30 VA
$R_{burden}$	0.5 Ohm
Class	5p20

### 3. Power System Description

The single line diagram of power system under study is shown in Fig. 2. The system parameters are obtained from

### 4. Simulation Results

An internal fault ( $F_1$ ) was considered inside the busbar protective zone assuming that short circuit is temporary

and not resistive. Another fault ( $F_2$ ) was considered outside the busbar protection zone as shown in Fig. 2. The relay's CTs orientation is built for busbar protection. The current signals, from ATP software, generated at sampling rate of 100 samples per cycle, this gives a sampling frequency of 5 KHz. The total simulation time is 0.2 Sec (i.e. the total number of samples is 1000). The fault inception time is 0.042 Sec (at sample 210) from the beginning of simulation time. The developed technique was applied by calculating the alienation coefficient between two corresponding quarter-cycles of input and output phase current signals of the protected busbar, where protective relays would normally be installed. The proposed technique is able to discriminate between the two types of two-phase faults either earthed or isolated; to confirm the two faulted phase type, another alienation coefficient is calculated between the two faulted phases currents. To implement the present technique, the studied power system configuration was simulated by using ATP software. The generated and measured three phase current signals of all feeders connected to the protected busbar are taken from the protective current transformers of busbar zone. Many simulation case studies are done to discriminate between the faulty phases and determine the fault location. These cases are done under effects of different pre-fault power level, fault resistance, and fault inception angle occurred in the simulated power system.

#### 4.1. Internal three Phase-to-Ground Fault (Case 1)

This case studies the performance of the proposed technique during the internal three phase-to-ground fault ( $A-B-C-G$ ) condition on the proposed technique. The operating conditions of the simulated power system are shown in Table 3. Figures 3(a-h) show the simulation results in case of internal three lines-to-ground fault. The figures show the three-phases secondary currents of the three feeders (generator, Load "1" and Load "2"), the input and output current signals of each phase for the protected busbar, calculated alienation coefficients ( $A_a$ ,  $A_b$  and  $A_c$ ) and trip signal of busbar protection, respectively. Figures 3(a-c) present the three-phase secondary current signals of the three feeders. Figures 3(d-f) show the input and output current signals of each phase for the protected busbar. In this case, it is noticed that the three phase currents during the fault are higher than the pre-fault currents and contains high DC component. The three-phase current correlation coefficients  $A_a$ ,  $A_b$  and  $A_c$  are shown in Figure 3(g). Each alienation coefficient is calculated between each two corresponding quarter-cycles of input and output phase current signals of the protected busbar. The values of  $A_a$ ,  $A_b$  and  $A_c$  are equal and close to zero before fault inception. At fault start and duration, they are greater than 0.1. From the above results, it is clear that the values of three alienation coefficients at fault initiation are good detector to determine the faulted phases and the zone of fault location; their values are closely to zero in case of normal operation and they are greater than  $A_x$  (where,  $A_x = 0.05$ ) in case of

internal fault condition. In this case, the fault location is internal and the faulted phases are  $A$ ,  $B$  and  $C$ . When the fault is internal, a trip signal is sent for busbar isolation from power system by opening all CBs of all feeders connected to the faulted busbar; the scheme sets trip signal to high (1) as shown in Figure 3(h).

Table 3. Operating conditions of electrical components

Electrical component (operating condition)	Data
$F_{operated}$	50 Hz
Load 1 (aux. load)	$10.85 + j 6.72 \text{ Ohm}$
Load 2 (aux. load)	$10.85 + j 6.72 \text{ Ohm}$
Load 3 (main load)	$8.5 + j 5.26 \text{ Ohm}$
Generator operating power angle ( $\delta_1$ )	0 Degree
Operating phase peak voltage of generator	16063 Volt
Generator grounding impedance	0.0 ohm

#### 4.2. Internal Single Line-to-Ground Fault (Case 2)

All parameters are kept as in case 1, except the fault type is changed from internal three lines-to-ground fault ( $A-B-C-G$ ) to internal single line-to-ground fault ( $A-G$ ). Figures 4(a-h) show the simulation results in case of internal single line-to-ground fault. The figures show the three-phases secondary currents of the three feeders (generator, Load "1" and Load "2"), the phase input and output current signals for the protected busbar, calculated alienation coefficients ( $A_a$ ,  $A_b$  and  $A_c$ ) and trip signal of busbar protection, respectively. Figures 4(a-c) present the three-phase secondary current signals of the three feeders. These figures show that the three phase currents during the fault are higher than the pre-fault currents and contains high DC component. Figures 4(d-f) show the input and output current signals of each phase for the protected busbar. The three-phase alienation coefficients  $A_a$ ,  $A_b$  and  $A_c$  are shown in Figure 4(g). Their values are equal and close to zero before fault inception. At fault start and duration,  $A_a$  is greater than 0.1 while  $A_b$  and  $A_c$  are nearly zero. From the above results, it is clear that the alienation coefficient value at fault initiation is good indicator to determine the faulted phase and the zone of fault location. In this case, the fault location is internal and the faulted phase is ( $A-G$ ). The occurrence of internal fault condition makes a trip signal is sent for busbar isolation from power system by opening all CBs of all feeders connected to the faulted busbar; the scheme sets trip signal to high (1) as shown in Figure 4(h).

#### 4.3. Internal Double Line-to-Ground Fault (Case 3)

This case studies the effect of internal double line-to-ground fault condition on the performance of the proposed algorithm. Therefore, all parameters are kept as in case 1, except the fault type is changed to internal double line-to-ground fault ( $A-B-G$ ). Figures 5(a-i) show the simulation results in case of internal double line-to-ground fault. The figures show the three-phases secondary currents of the three feeders (generator, Load "1" and Load "2"), the input and output current signals of each phase for the protected busbar, calculated alienation coefficients ( $A_a$ ,  $A_b$ ,  $A_c$  and

$A_{ab}$ ) and trip signal of busbar protection, respectively. Figures 5(a-c) present the three-phase secondary current signals of the three feeders. The three-phase current signals during the fault interval are higher than the pre-fault currents and with high DC component. Figures 5(d-f) show the input and output current signals of each phase for the protected busbar. The three-phase alienation coefficients  $A_a$ ,  $A_b$  and  $A_c$  are shown in Figure 5(g). The alienation coefficient  $A_{ab}$ , calculated between the two faulted phases currents ( $A$  and  $B$ ), is shown in Figure 5(h). The values of alienation coefficients  $A_a$ ,  $A_b$  and  $A_c$  are equal and close to zero before fault inception. At fault starts and duration,  $A_a$  and  $A_b$  are greater than the value of 0.1, whereas  $A_c$  is nearly zero. From the above results, it is clear that the alienation coefficients values  $A_a$ ,  $A_b$  and  $A_c$  at fault initiation can define the faulted phases ( $A$  and  $B$ ). At fault start, the alienation coefficient  $A_{ab}$  has a value of 0.45 (i.e. the value  $A_{ab}$  is not equal to zero). The alienation coefficients values ( $A_a$ ,  $A_b$ ,  $A_c$  and  $A_{ab}$ ), at fault start, confirm that the fault type is double line-to-ground fault. Before fault inception, the value of alienation coefficient  $A_{ab}$  is equal to  $1 - (\cos(120^\circ))^2 = 0.75$ , which is considered a normal value. From the obtained results, it is clear that the alienation coefficient value at fault initiation is good detector to determine the faulted phase and fault location zone. In this case, the fault location is internal and the faulted phases are ( $A$ - $B$ - $G$ ). The event of internal fault condition leads to a trip signal is sent for isolation of the faulted busbar by opening all CBs of all feeders connected to this busbar; the scheme sets trip signal to high (1) as shown in Figure 5(i).

#### 4.4. Internal Double Line Fault (Case 4)

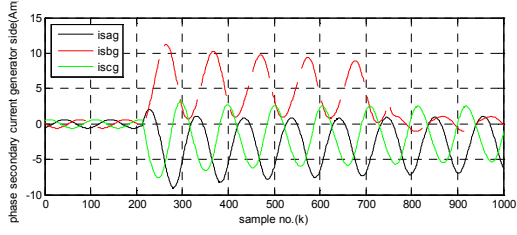
This case studies the effect of internal double line fault Condition on the performance of the proposed algorithm. Therefore all parameters are kept as in case 1, except that the fault type is changed to internal double line fault ( $A$ - $B$ ). Figures 6(a-i) show the simulation results in case of internal double line fault. The figures show the three-phases secondary currents of the three feeders (generator, Load "1" and Load "2"), the input and output current signals of each phase for the protected busbar, calculated alienation coefficients ( $A_a$ ,  $A_b$ ,  $A_c$  and  $A_{ab}$ ) and trip signal of busbar protection, respectively. Figures 6(a-c) present the three-phase current signals of the three feeders. The three-phase current signals during the fault interval are higher than the pre-fault currents and with high DC component. Figures 6(d-f) show the input and output current signals of each phase for the protected busbar. The three-phase alienation coefficients  $A_a$ ,  $A_b$  and  $A_c$  are shown in Figure 6(g). The alienation coefficient  $A_{ab}$ , calculated between the two faulted phases currents ( $A$  and  $B$ ), is shown in Figure 6(h). The values of alienation coefficients  $A_a$ ,  $A_b$  and  $A_c$  are equal and close to zero before fault inception. At fault starts and duration,  $A_a$  and  $A_b$  are greater than the value of 0.1, whereas  $A_c$  is nearly zero. At fault start and duration,

the alienation coefficient  $A_{ab}$  has a value of zero, whereas its value is normal and equal to 0.75 before fault inception. The values of alienation coefficients ( $A_a$ ,  $A_b$ ,  $A_c$  and  $A_{ab}$ ), at fault inception, confirms that the fault type is phase-to-phase fault. Consequently, our technique can determine the fault type whether double phase-to-ground or phase-to-phase by the alienation coefficient  $A_{ab}$  calculated between the two faulted phase's currents; If  $A_{ab} \approx$  zero, at fault starts, the fault type is phase-to-phase otherwise it is double phase-to-ground. From the obtained results, it is clear that the alienation coefficient values, at fault initiation, are good detector to determine the faulted phases, distinguish between phase-phase isolated and grounded faulty and discriminate fault location zone without adding any extra measuring equipments. In this case, the fault location zone is internal and the faulted phases are ( $A$ - $B$ ). The internal fault condition leads to a trip signal sent for isolation of the faulted busbar by opening all CBs of all feeders connected to this element; the scheme sets trip signal to high (1) as shown in Figure 6(i).

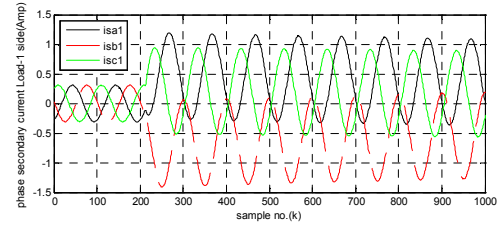
#### 4.5. External Single Line-to-Ground Fault with CT Saturation (Case 5)

All parameters are kept as in case 1, except the burden resistance ( $R_{burden}$ ) for phase "A" current transformer of load "1" feeder is changed from 0.5 Ohm to 110 Ohm. Figures 7(a-h) show the simulation results in case of external single line-to-ground fault with CT saturation. The figures show the three-phases secondary currents of the three feeders (generator, Load "1" and Load "2"), the input and output current signals of each phase for the protected busbar, calculated alienation coefficients ( $A_a$ ,  $A_b$  and  $A_c$ ) and blocking trip signal of busbar protection, respectively. Figures 7(a-c) present the three-phase secondary current signals of the three feeders. The three-phase current signals during the fault interval are higher than the pre-fault currents and with high DC component. Figures 7(d-f) show the input and output current signals of each phase for the protected busbar. The three-phase alienation coefficients  $A_a$ ,  $A_b$  and  $A_c$  are shown in Figure 7(g). Their values are equal and close to zero before fault inception. From the instant of fault start to the instant of CT saturation start,  $A_a$  is also close to zero. The coefficient  $A_a$  becomes greater than 0.05 during the saturated portion and it is less than 0.05 during the unsaturated portion of each cycle for current signal; while  $A_b$  and  $A_c$  are nearly zero through the period of fault interval. From the above results, it is clear that the alienation coefficient values from fault initiation to CT saturation occurrence are good supervisor to determine the fault location zone in case of CT saturation condition. In this case, the fault location zone is external because of alienation coefficient value  $A_a$  is close to zero during the free saturated portion of current signal. Due to the occurrence of external fault condition, the scheme holds trip signal to low (0) as shown in Figure 7(h).

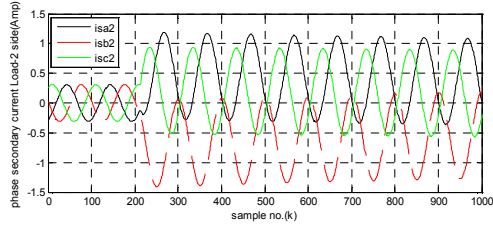




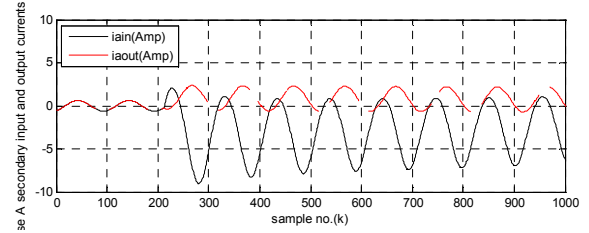
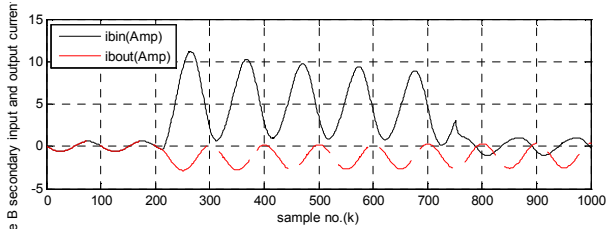
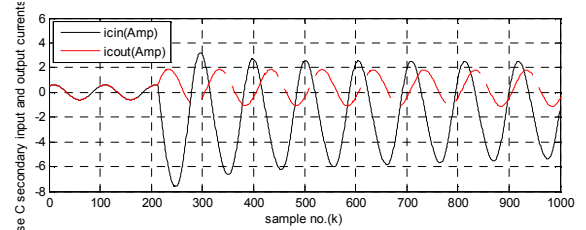
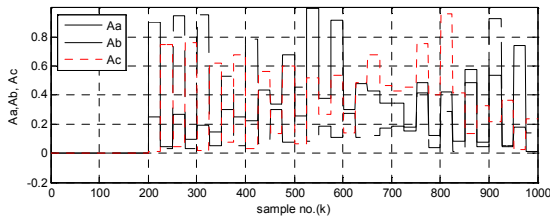
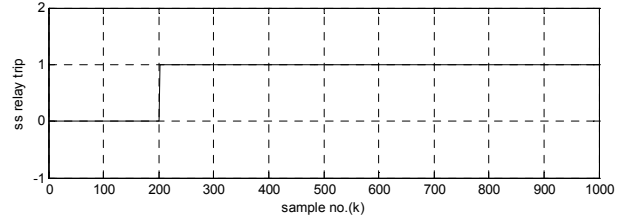
(a) Three phases instantaneous secondary currents of Generator feeder.



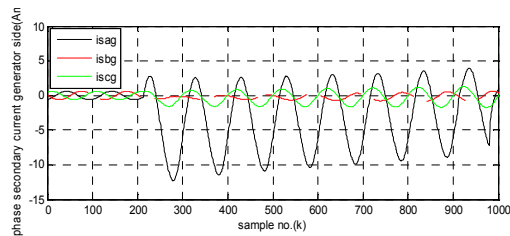
(b) Three phases instantaneous secondary currents of Load 1 feeder.



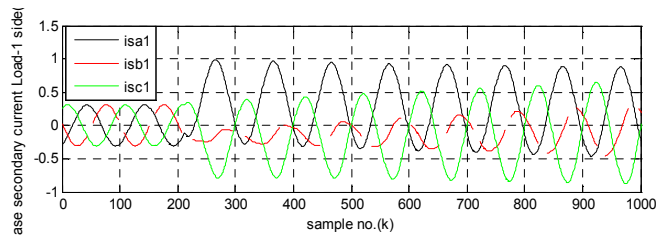
(c) Three phases instantaneous secondary currents of Load 2 feeder.

(d) The two input and output current signals for phase "A", ( $i_{a1}$  and  $i_{a2}$ ).(e) The two input and output current signals for phase "B", ( $i_{b1}$  and  $i_{b2}$ ).(f) The two input and output current signals for phase "C", ( $i_{c1}$  and  $i_{c2}$ ).(g) Alienation coefficients  $A_a$ ,  $A_b$  and  $A_c$ .

(h) Trip signal of busbar protection.

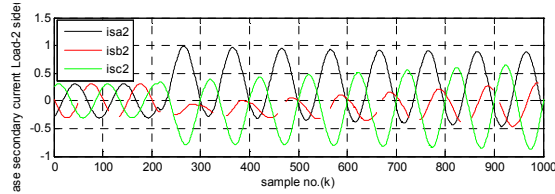
**Figures 3(a-h) Simulation Results in case of Internal Three-Line-to-Ground Fault.**

(a) Three phases instantaneous secondary currents of Generator feeder.

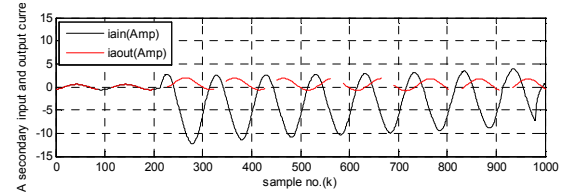
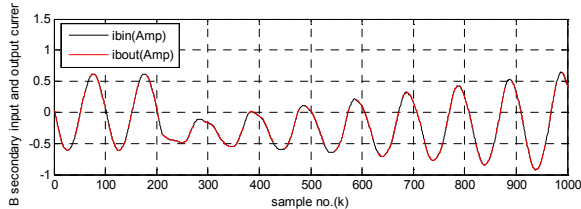
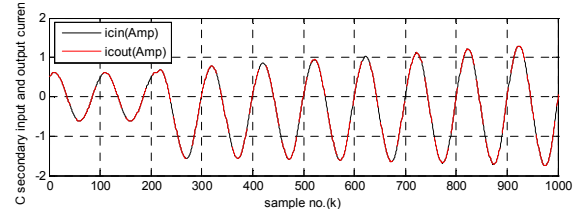
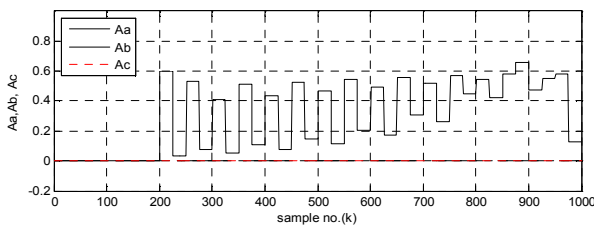
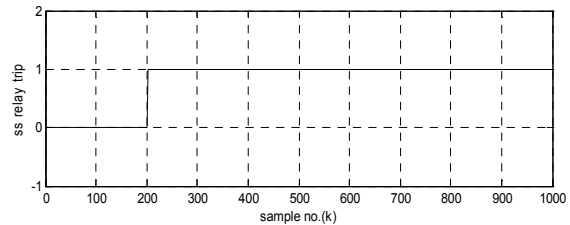


(b) Three phases instantaneous secondary currents of Load 1 feeder.

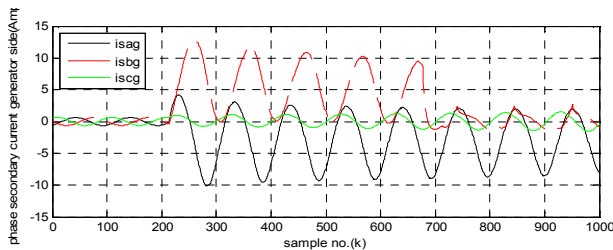




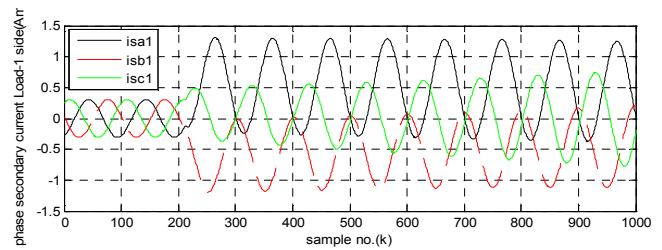
(c) Three phases instantaneous secondary currents of Load 2 feeder.

(d) The two input and output current signals for phase "A", ( $i_{a1}$  and  $i_{a2}$ ).(e) The two input and output current signals for phase "B", ( $i_{b1}$  and  $i_{b2}$ ).(f) The two input and output current signals for phase "C", ( $i_{c1}$  and  $i_{c2}$ ).(g) Alienation coefficients  $A_a$ ,  $A_b$  and  $A_c$ .

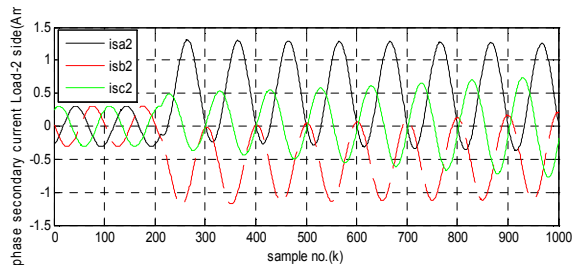
(h) Trip signal of busbar protection.

**Figures 4(a-h) Simulation Results in case of Internal Single Line-to-Ground Fault.**

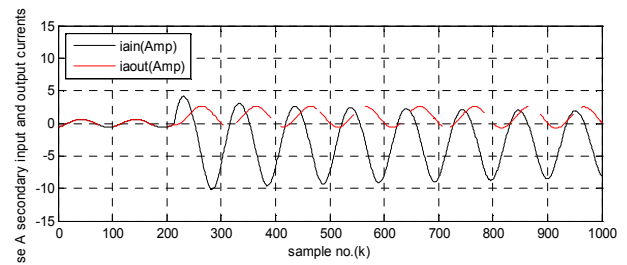
(a) Three phases instantaneous secondary currents of Generator feeder.

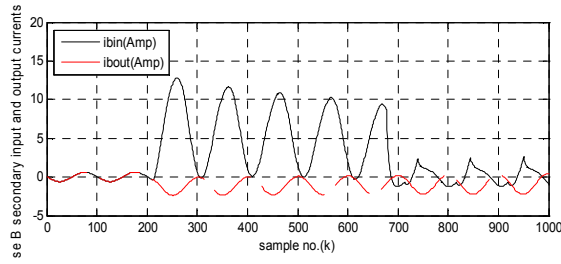
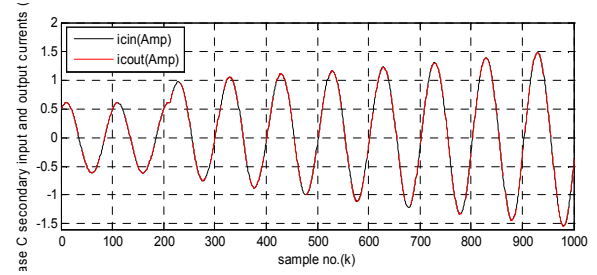
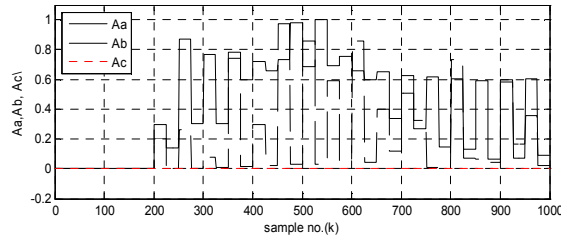
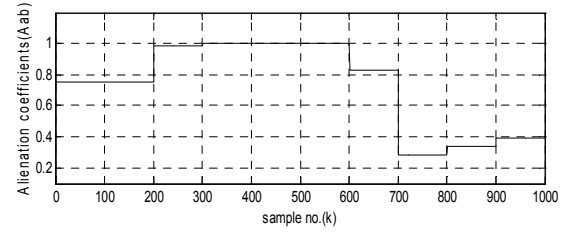
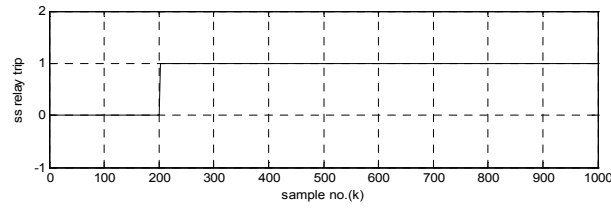


(b) Three phases instantaneous secondary currents of Load 1 feeder.

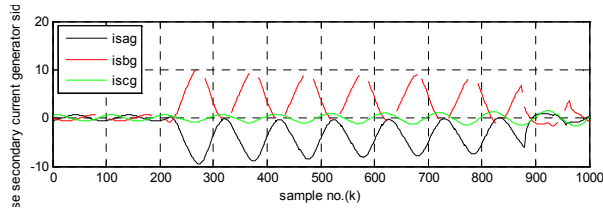


(c) Three phases instantaneous secondary currents of Load 2 feeder.

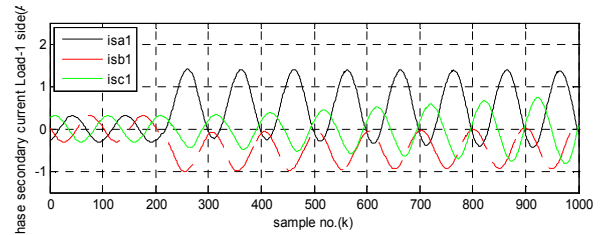
(d) The two input and output current signals for phase "A", ( $i_{a1}$  and  $i_{a2}$ ).

(e) The two input and output current signals for phase "B", ( $i_{b1}$  and  $i_{b2}$ ).(f) The two input and output current signals for phase "C", ( $i_{c1}$  and  $i_{c2}$ ).(g) Alienation coefficients  $A_a$ ,  $A_b$  and  $A_c$ .(h) Alienation coefficients  $A_{ab}$ .

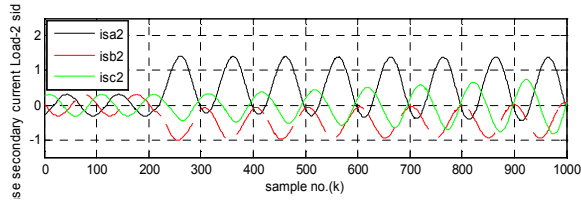
(i) Trip signal of busbar protection.

**Figures 5(a-i) Simulation Results in case of Internal Double Line-to-Ground Fault.**

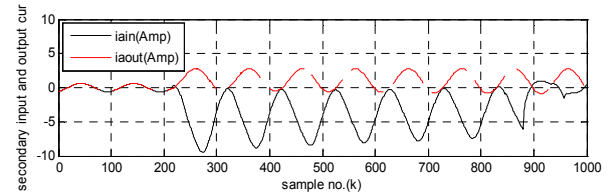
(a) Three phases instantaneous secondary currents of Generator feeder.

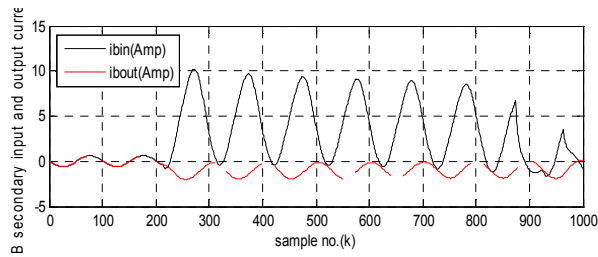
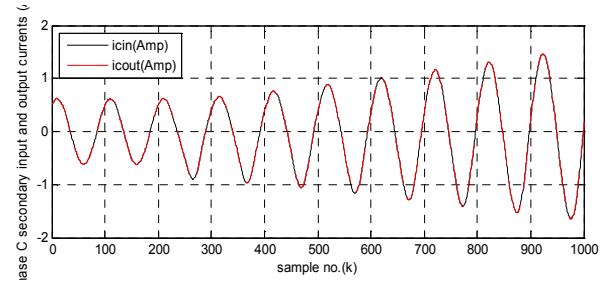
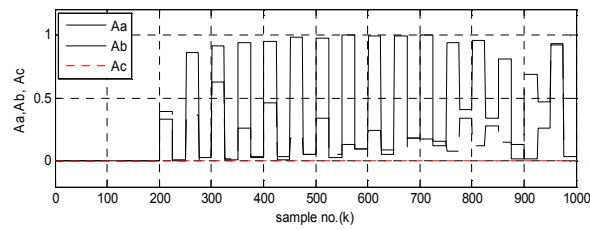
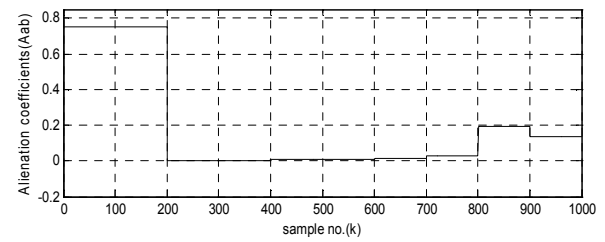
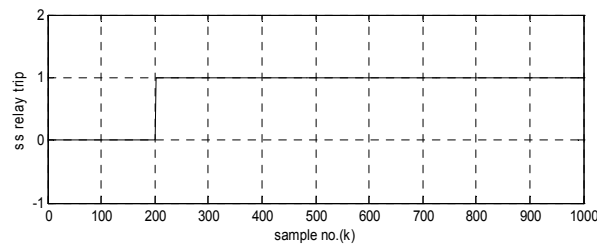


(b) Three phases instantaneous secondary currents of Load 1 feeder.

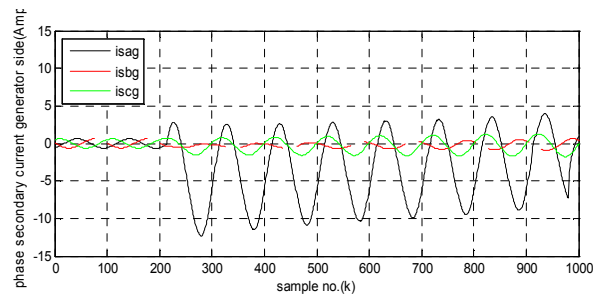


(c) Three phases instantaneous secondary currents of Load 2 feeder.

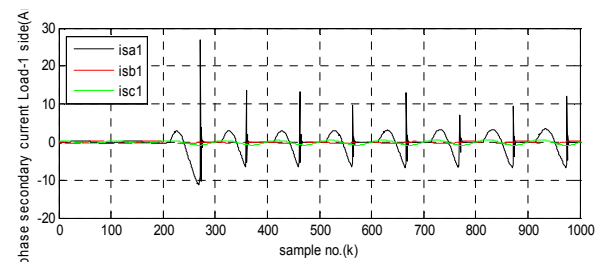
(d) The two input and output current signals for phase "A", ( $i_{a1}$  and  $i_{a2}$ ).

(e) The two input and output current signals for phase "B", ( $i_{b1}$  and  $i_{b2}$ ).(f) The two input and output current signals for phase "C", ( $i_{c1}$  and  $i_{c2}$ ).(g) Alienation coefficients  $A_a$ ,  $A_b$  and  $A_c$ .(h) Alienation coefficients  $A_{ab}$ .

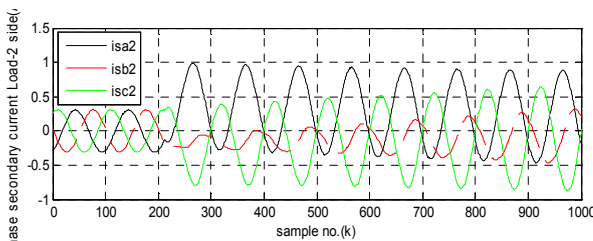
(i) Trip signal of busbar protection.

**Figures 6(a-i) Simulation Results in case of Internal Double Line Fault.**

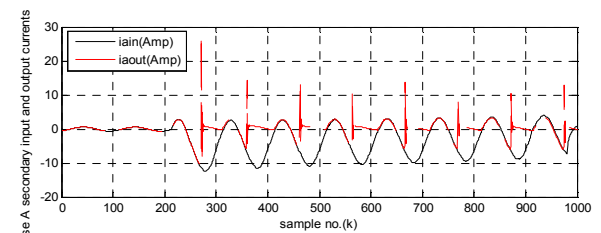
(a) Three phases instantaneous secondary currents of Generator feeder.

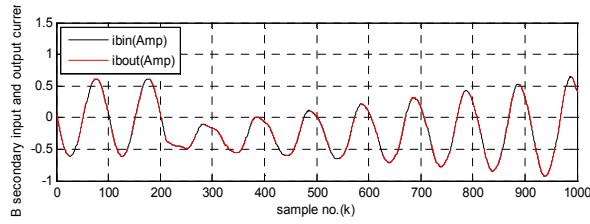
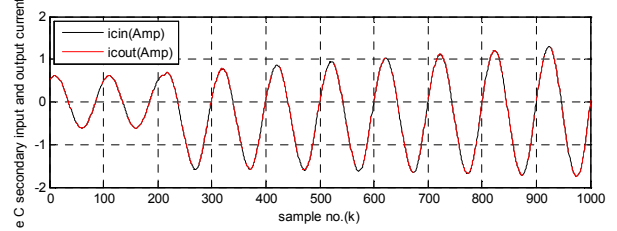
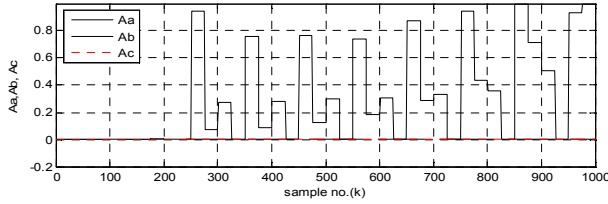
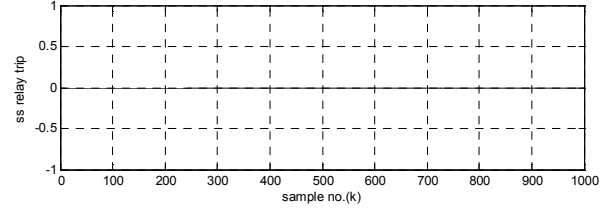


(b) Three phases instantaneous secondary currents of Load 1 feeder.



(c) Three phases instantaneous secondary currents of Load 2 feeder.

(d) The two input and output current signals for phase "A", ( $i_{a1}$  and  $i_{a2}$ ).

(e) The two input and output current signals for phase "B", ( $i_{b1}$  and  $i_{b2}$ ).(f) The two input and output current signals for phase "C", ( $i_{c1}$  and  $i_{c2}$ ).(g) Alienation coefficients  $A_a$ ,  $A_b$  and  $A_c$ .

(h) Blocking trip signal of busbar protection.

**Figures 7(a-h)** Simulation Results in case of External Single Line-to-Ground Fault with CT saturation.

## 5. Conclusions

In this paper, a reliable and efficient technique has been presented for busbar protection by using alienation algorithm. ATP software has been used for generating fault data and then processed in MATLAB to get an alienation coefficient between input and output currents for each phase of busbar. The three-phase coefficients are used in the proposed algorithm to implement relay logic. Results of case studies for different types of faults are presented. Case study results show that the technique used correctly detects faults, determines the fault location, selects faulty phase and discriminates external fault with CT saturation.

The main achievements of this work are as follows:

1. Introduced a new technique for protecting busbar, against fault conditions, based on alienation coefficients
2. The technique does not use the power system element data as it needs only measuring the three-phase currents of each feeder connected to the protected busbar.
3. It is accurate to identify all ten types of short-circuit fault conditions in busbar protection zone.
4. Fast method, as the time taken by this method is about 10 ms (for a 50-Hz system).
5. The reliability of the proposed method is quite high.
6. It is quite effective over a wide range of a pre-fault power level, fault resistance and fault inception angle.
7. The effects of DC components and harmonics are eliminated with estimation of alienation coefficients.
8. The suggested alienation technique is characterized by being simple, fast, reliable and accurate and can be implemented practically, thus it can be used as a base for implementing a cheap and reliable digital protective relay against internal faults for busbar.
9. Control of algorithm operation speed by selecting correlated window in correlation and alienation calculations, this mean adjustable speed (quarter, half or one-cycle).

10. Control of proposed algorithm sensitivity (pick up value of alienation) by selecting alienation setting and correlated window.

## References

- [1] IEEE Guide for the Application of Current Transformers Used for Protective Relaying Purposes IEEE Std. C 37.110-1996.
- [2] Working group of the Relay Input Sources Subcommittee of the Power System Relaying Committee "Transient response of current transformers" IEEE Transaction on power apparatus and systems, Vol. PAS-96, no. 6, November/December 1977.
- [3] W.J. Smolinsky "Design Consideration in the Application of Current Transformers For Protective Relaying Purposes", IEEE Transactions on Power Apparatus and System, Vol. PAS-92, no.4, July/August 1973.
- [4] D.A. Bradley, C.B.Gray, D.O'Kelly "Transient compensation of current transformers" IEEE Transactions on Power Apparatus and Systems, Vol. PAS-97, no.4, July/Aug 1978
- [5] Y.C. Kang, J.K.Park, S.H.Kang, A.T. Johns, R.K. Aggarawal " An algorithm for compensating secondary currents of current transformers" IEEE Transactions on Power Delivery, Vol.12, no.1, January 1997
- [6] D.C.Yu, Z.Wang, J.C. Cummins, H.-J. Yoon, L.A.Kojovic, and D.Stone "Neural network for current transformer saturation correction" in proc. IEEE Transm. Distrib. Conf., New Orleans, LA, Apr.1999.
- [7] M.E. Masoud, E.H.Shabab-Eldin, M.M Eissa, and M.F.Elnagar. "A New compensating secondary current technique for saturated current transformers" The 8<sup>th</sup>International Middle- East power system conference "MEPECON 2001", PP549-555.

- [8] Jiuping Pan, Khoi Vu, and Yi Hu "An Efficient Compensation Algorithm for Current Transformer Saturation Effects" IEEE Transactions on Power delivery, Vol. 19, no.4, October, 2004, PP1623-1628.
- [9] M.A. Salem, M.I. Gilany, Z. Osman and E. about Zahab "A new algorithm for compensating the secondary current during current transformer saturation" The tenth International Middle- East power systems conference "MEPECON 2005" PP 427-433.
- [10] M.S. Sachdev, T.S. Sidhu, H.S. Gill, "A busbar protection technique and its performance during CT saturation and CT ratio-mismatch", Power Delivery, IEEE Transactions on (Volume:15, Issue: 3 ), Page(s):895 - 901, Jul 2000.
- [11] Xuyang Deng, Jiale Suonan, Zaibin Jiao and Xiaoning Kang, "A Model Parameter Identification Based Bus-bar Protection Principle", Power and Energy Engineering Conference (APPEEC), 2010 Asia-Pacific, Page(s):1 – 6, March 2010.
- [12] Jiale Suonan, Xuyang Deng and Guobing Song, "A Novel Busbar Protection Based on Fault Component Integrated Impedance", Power and Energy Engineering Conference (APPEEC), 2010 Asia-Pacific, Page(s):1 – 6, March 2010.
- [13] Libao Xu, Grasset, H., Xingli Dong, Chenliang Xu and Ruidong Xu, "A new method for busbar protection stability improvement", Developments in Power System Protection (DPSP 2010). Managing the Change, 10th IET International Conference on, Page(s):1-4, April 2010.
- [14] ATP - version 3.5 for Windows 9x/NT/2000/XP - Users' Manual Preliminary Release No. 1.1 - October 2002.
- [15] W. Hauschild, and W. Mosch, "Statistical Techniques for High Voltage Engineering", hand book, English edition published by peter pere grinus Ltd., London, United Kingdom, chapter 2, pp. 78-79, 1992.
- [16] Edwards, A. L. "The Correlation Coefficient." Ch. 4 in an Introduction to Linear Regression and Correlation. San Francisco, CA: W. H. Freeman, pp. 33-46, 1976.
- [17] Snedecor, G. W. and Cochran, W. G. "The Sample Correlation Coefficient  $r$  and Properties of  $r$ ." 10.1-10.2 in Statistical Methods, 7th ed. Ames, IA: Iowa State Press, pp. 175-178, 1980.
- [18] Press, W. H.; Flannery, B. P.; Teukolsky, S. A.; and Vetterling, W. T. "Linear Correlation", Cambridge, England: Cambridge University Press, pp. 630-633, 1992.
- [19] Spiegel, M. R. "Correlation Theory." Ch. 14 in Theory and Problems of Probability and Statistics, 2nd ed. New York: McGraw-Hill, pp. 294-323, 1992.
- [20] Instruction Manual for Generator Electrical Equipment, Upper Egypt Electricity Production Company, Elkureimat II 750 MW Combined Cycle Project, Steam Turbine Generator & Auxiliaries (Generator Electrical Equipment), Hitachi, Ltd., Tokyo Japan, 2006.